

Liquid-Solid Phase Transition and the Change of the Frictional Force of the System with Two particles in a Box.

Akinori Awazu*

Department of Mathematical Sciences

Osaka Prefecture University, Sakai 599-8531 Japan.

Abstract

Liquid-solid phase transition and the change of the frictional force of a system with two hard spheres in a two-dimensional rectangular box are discussed. Under controlling the pressure or the supply of energy from the wall, the solid like state, the solid-liquid temporal coexistence state, and the liquid like state are alternatively observed. The frictional force which works on particles and the mobility of the system are measured under the supply of the energy with an asymmetric external force. Characters of frictional forces for the 0 mobility state and that for the large mobility state are obtained like, respectively, that of the static and the dynamic frictions of solid-on-solid system. The strong temperature dependency is also observed in the profile of the relation between the above frictional force and the mobility. From above results, the relation between the friction and the velocity of a plate on granular layers which includes the hysteresis loop [S.Nasuno et al., Phys. Rev. Lett **79** (1997) 949 et. al.] is discussed. PACS number(s):

The appearance of the static friction and the dynamic friction, and the change between them are familiar and important subjects of fundamental physics. They are universal phe-

*E-mail: awa@zenon.ms.osakafu-u.ac.jp

nomena which are usually observed at surfaces of macro-scale objects. From the microscopic point of view, the change between above two types of frictions is expected to have close relationship with the liquid-solid phase transition around surfaces¹⁻⁵. Here, the liquid-solid phase transition in this case is caused by variances of external driving forces like shear forces, which means that this transition occurs under non-equilibrium states. By numerical simulations of systems containing $10^{1\sim 4}$ hard or soft core particles, the liquid-solid phase transition with a Van der Waals loop was observed⁶⁻¹⁰. Very similar relations were observed also in the system with two hard spheres in a rectangular box¹¹. Moreover, this system showed not only the solid-liquid phase transition but also the transition like glass transition with the appearance of α and β like relaxation and the disappearance of the Van der Waals loop. From these facts, we can expect that the appearances of above phase transitions are universal characters caused by the effect of the excluded volume independent of the number of associating particles. In this paper, we try to discuss the appearance of the static and the dynamic frictions and the change between them through a simple model with a few modifications of that introduced in the previous paper¹¹. First, phase transitions of the system under equilibrium and non-equilibrium states by controlling the supply of energy and the pressure in horizontal direction, are investigated. This controlled pressure corresponds to the normal reaction in the general treatment of friction. Based on these investigation, characteristic features of frictional forces in this system are discussed.

The system of our considerations consists of two-dimensional hard sphere particles with unit mass and unit radius which are confined in a two-dimensional rectangular box (Fig. 1). The right wall with unit mass of the box can move in the horizontal direction. The position of the right wall is $X(t)$ ($X(t) > 2$) and the constant force $-f$ is working on this wall in the horizontal direction. The left wall is set at the origin of the horizontal axis and are connected to the energy source. The bottom of the box is set at the zero height of the vertical direction, and the position of the top of the box (the box height) is Y ($Y > 4$). All walls are rigid, and interactions between two particles, and, between a particle and a wall without energy sources, are only through hard core collisions. These tasks are implemented

in the following manner; the tangential velocities to the collision plane are preserved, while the normal component of relative velocity Δv_n changes into $-\Delta v_n$. A particle hitting the left wall connected to the energy source with the velocity (v_h, v_v) bounces back with the velocity (V_h, V_v) ($V_h > 0$). Here, subscripts h and v indicate, respectively, the horizontal and the vertical direction. The velocity (V_h, V_v) is chosen randomly from the probability distributions $P_h(V_h)$ and $P_v(V_v)$ ¹²

$$P_h(V_h) = T^{-1} V_h \exp\left(-\frac{V_h^2}{2T}\right) \quad (1)$$

$$P_v(V_v) = (2\pi T)^{-\frac{1}{2}} \exp\left(-\frac{(V_v - U)^2}{2T}\right) \quad (2)$$

where T is the temperature of the energy source. (We give the Boltzmann constant as 1.) The case with $U \neq 0$ means the asymmetric force working on the system from the energy source in vertical direction. We only consider the case of $Y > 4$ which means these two particles can exchange their positions in horizontal direction with each other. When $X(t) > 4$, these spheres can exchange their positions in vertical direction. On the contrary, these particles cannot exchange their positions in vertical direction when $X(t) < 4$. In the previous paper, we fixed $X(t) = X$ and defined the state with $X > 4$ as the liquid state and that with $X < 4$ as the solid state¹¹. In this paper, however, because we will treat probability distributions of $X(t)$ in the following discussions, we slightly modify definitions of these states as follows; The solid state is defined as the state in which the probability distribution of $X(t)$ has a peak at $X(t) < 4$, and the liquid state is defined as the state in which the distribution has a peak at $X(t) > 4$.

First, we focus on the cases of $U = 0$ which are the same as the situation that a heat bath is connected to the left wall. Figure 2 is the probability distribution of the position of right wall $X(t)$ for, respectively, when (a) $Y = 4.5$, (b) $Y = 5.0$, and (c) $Y = 5.5$ for typical values f under the same temperature T ($= 0.1$). Independent of Y , each distribution has only one peak at $X(t) < 4$ for large value of f (solid state), or $X(t) > 4$ for small value of f (liquid state). For middle values of f , however, each distribution has two peaks for

the case of $Y \leq 5.0$; One of them is at $X(t) < 4$ and the other is at $X(t) > 4$ (Fig. 2 (a)). This indicates, in the present situation, the system passes between the liquid state and the solid state. Thus, the discontinuous transition between the solid state and the liquid state appears like in the system with many hard spheres⁸. These two peaks become blunt with the increase of Y , and the probability distribution around $X(t) = 4.0$ becomes almost flat for $Y \sim 5.0$ (Fig. 2 (b)). Differently from the case of $Y \leq 5.0$, each distribution has always only one peak in the case of $Y > 5.0$ (Fig. 2 (c)), where this peak crosses the line $X = 4$ with no singularities for the middle f . The appearance and the disappearance of the discontinuous transition are considered to be strongly related to those of Van der Waals loop which were observed when the width of the box is fixed¹¹. However, the height with no discontinuous transition is $Y > Y^* \sim 5.0$, while the one with no Van der Waals loop is $Y' > Y'^* \sim 6.0$ in our previous paper¹¹. Our value Y^* is, if anything, similar to another critical height $Y'_c \sim 5.0$ for the previous model, where β and α like relaxations appear for $Y' \geq Y'_c$ ¹¹. If we fix the value f and change the value $\beta = 1/T$, we observe qualitatively the same results as the above.

Next, we discuss the cases with $U > 0$. In these cases, the system becomes non-equilibrium because of the asymmetric force working on particles in vertical direction along the left wall. Figure 3 is the probability distribution of the position of the right wall $X(t)$ for, respectively, when (a) $Y = 4.5$ with low temperature ($T = 0.1$), (b) $Y = 4.5$ with high temperature ($T = 0.4$), (c) $Y = 5.5$ with low temperature ($T = 0.1$), and (d) $Y = 5.5$ with high temperature ($T = 0.4$), for typical values U under constant value $f (= 1)$. Here, we set T with which the probability distribution of $X(t)$ has only one peak for $X(t) < 4$ (the solid state is realized) for the case of $U = 0$. The discontinuous phase transition between the solid state and the liquid state with the liquid-solid temporal coexistence state is realized for $Y \leq 5.0$ by varying the value U (Fig. 3 (a) and (b)). Differently from cases of the previous discussions with $U = 0$, however, such a discontinuous phase transition is observed also for cases with $Y > 5.0$. In these situations, two particles are compressed near the top wall of the box by the asymmetric force with $U > 0$. This means the region in which particles spend

almost all the time becomes smaller in vertical direction. Then, the Y -dependent characters of the phase transition become blunt. With increase of T and Y , these two peaks become smoother and the top of the probability distribution of $X(t)$ for middle U comes close to be flat (Fig. 3(d)).

Now, we define the mobility m of the system as the average frequency of the change of sign of δy . Here, δy is the relative position between two particles in vertical direction. The solid state is realized when $m = 0$, and the liquid state is realized when m is large. From the asymmetric force characterized by the velocity U , the force $F_{ex} = \lim_{t \rightarrow \infty} \frac{1}{t} (\sum_{col} (V_v - v_v))$ works on particles at the left wall in average. Here, \sum_{col} is the sum of individual collisions between the left wall and particles. Figure 4 is the relation between (a) U and m , and (b) U and F_{ex} for typical values T under constant values $f = 1$ and $Y = 5.0$. For small U , $m = 0$ and $F_{ex} \propto U$ are realized, and $m \propto U$ and $F_{ex} = constant$ are realized for large U . Here, F_{ex} for each U becomes large with T decreasing, although T dependencies of F_{ex} are small for large U . Moreover, each U - F_{ex} curve for small T has a peak which disappears for large T . When the width of the box becomes larger, m become larger. Then, frequency of collisions between particles and the left wall connected to energy source decreases. These facts make F_{ex} to be almost constant for large m although U increases. Figure 5 indicates relations between m and F_{ex} by increasing U for typical values T under constant values $f = 1$, where (a) $Y = 5.0$ and (b) $Y = 4.5$. Here, each state of the system is almost stationary in which m looks constant if averaged over the macroscopic time scale sufficiently larger than the mean free time of particles. Then, F_{ex} is regarded as the driving force to keep each steady state. This also means that the effective frictional force R , the magnitude of which is equal to that of F_{ex} , emerges in the system to inhibit the mobilization of the system. Hence, Fig. 5 also indicates the relations between the mobility m and the frictional force R . Here, f plays a role of the normal reaction of this system which is treated as the constant 1. Thus, the relations between m and R are equivalent to those of m and the effective friction coefficient $\mu = \frac{R}{f}$. In Fig. 5, for small T , R has a maximum value at a neighborhood of $m = 0$, and this decreases monotonically and becomes almost constant with the increase of

m . These characteristics of m - R relation are similar to those of velocity-friction relations of solid-on-solid system which satisfies Coulomb-Amontons's frictions laws¹. For large T , on the contrary, R increases monotonically and becomes almost constant value with the increase of m different from Coulomb-Amontons's frictions laws. When Y become small, R increases a little with m for large m (Fig. 5 (b)). However, this increase is small, and qualitative characteristics obtained in the above are considered to be independent of Y .

Figure 6 is the relations between, respectively, (a) m and the friction coefficient $\mu = \frac{R}{f}$, and (b) f and μ by increasing f for typical values T under a constant value U ($Y = 5.0$). In this case, the liquid state with large m and the solid state with $m = 0$ are realized for, respectively, small f and large f . In cases with $U = 0$, large f states are equivalent to small T states. Hence, it is natural that profiles of the relations for small m in Fig. 6 (a) become similar to those of relations with small T in Fig. 5. Because of the same reason, the probability distribution of $X(t)$ for large f also behaves similarly to those with small T in Fig. 3. In Fig. 6 (a), μ of the $m = 0$ states is obtained which is larger than μ of the large m state. Moreover, μ remains constant independently of m for large m . In Fig. 6 (b), the derivative $\frac{d\mu}{df}$ is small if f is small or large. This means the frictional force is almost proportional to the normal reaction in these region. These characteristics are also similar to those of solid-on-solid frictions which satisfy Coulomb-Amontons's frictions laws¹. In Fig. 6 (b), for middle f , friction coefficients for each T increase with the increase of m . With the decrease of T , the friction constant increases sharply.

Now, we focus on the relation between the velocity of a plate on granular layers and the friction between the plate and granular layers^{3,4}. Recently, from a sensitive experiment, Nasuno et al. found that the relation between the plate velocity and the frictional force makes a hysteresis loop³; The frictional force is multi-valued, which is less for decreasing velocity to 0 than for increasing velocity from 0. It is remarkable that a loop, which looks very similar to above one, can be created by combining m - R relations for large and small T (see Fig. 5). Thus, we try to understand qualitatively the mechanism of history dependencies of velocity-friction relations on granular layers from the m - R relations in Fig. 5. Here, m

corresponds to plate velocity and R corresponds to friction on granular layers. We assume that the granular temperature T_g of the surface of granular layers plays similar roles to the temperature of energy source in our system. Here, T_g is defined as the half of the mean-square of velocity fluctuation of each granular particle. Initially, the plate and each particle in granular layers do not move, where $T_g = 0$. Soon after the plate starts slipping, T_g increases but it is expected to be small at the early stage. Hence, the frictional force decreases with increasing the plate velocity on granular layers like m - R relations with small T in Fig. 5. When plate moves faster, however, T_g is expected to become large because the plate excites each particle in granular layers. Then, the frictional force is almost constant for finite plate velocity like m - R relations with middle or large T in Fig. 5. By this friction, in the final stage, the plate stops and T_g becomes 0 again. Thus, in this granular system, T_g varies with time and this variance of T_g iterates all along because the plate is pushed continuously. This iteration and the temperature dependency of the frictional force explain the appearance of such a hysteresis loop in granular materials.

In this paper, we discussed the liquid-solid phase transition and the occurrence of static and dynamic frictions of the system with two particles in a rectangular box. First, we discussed the liquid-solid phase transition by controlling the pressure in horizontal direction or the temperature of a heat bath. When the height of the box is small, the discontinuous liquid-solid phase transition with the appearance of the liquid-solid temporal coexistence was observed. However, the liquid-solid phase transition becomes continuous when the height of the box is higher than a critical value. Next, we discussed the relation between the mobility and the frictional force of the system in which particles are excited by an asymmetric force in the vertical direction. In the simulation, we observed the frictional forces which are quite similar to the static friction and the dynamic friction observed in solid-on-solid system. Moreover, we found that the relation between these frictional forces and the mobility strongly depends on the temperature of the heat bath. Taking these characteristics into consideration, we discussed the origin of the hysteresis loop in the granular friction. Our discovery of temperature dependency of these characters of frictions is an important result

of our simulation. More discussions together with theoretical, numerical, and experimental studies are needed in the future. Also the analytical study of dynamical properties of frictional forces on granular layers is left as an important issue.

The author is grateful to H.Nishimori, K.Sekimoto, S.Nasuno, and S.Yukawa for useful discussions. This research was supported in part by Grant-in-Aid for JSPS Felows 10376.

REFERENCES

1. H. Matsukawa, *Mathematical Science* **433** (2000) 41 (in Japanese); V. Zaloji, M. Urbakh and J. Klafter, *Phys. Rev. Lett.* **81** (1998) 1227; E. Granato and S.C. Ying, *Phys. Rev. Lett.* **85** (2000) 5368
2. F. Heslot, T. Baumberger, B. Perrin, B. Caroli, and C. Caroli, *Phys. Rev. E* **49** (1994) 4973;
3. S. Nasuno, A. Kudrolli, and J.P. Gollub, *Phys. Rev. Lett* **79** (1997) 949; S. Nasuno, A. Kudrolli, A. Bak and J.P. Gollub, *Phys. Rev. E.* **58** (1998) 2161
4. P.A. Thompson and G.S. Grest, *Phys. Rev. Lett.* **67**, 1751 (1991); J.M. Carlson and A.A. Batista, *Phys. Rev. E* **53** (1996) 4153; H. Hayakawa, *Phys. Rev. E.* **60** (1999) 4500; H. Hayakawa, *Prog.Theo. Phys.Suppl*
5. A. Subbotin, A. Semenov and M. Doi, *Phys. Rev. E* **56** (1997) 623 ;K. Sato and A. Toda, *J.Phys.Soc.Jpn* **68** (1999) 77
6. W.W. Wood and J.D. Jacobson, *J. Chem. Phys* **27** (1957) 1207; B.J Alder and T.E Waiwright, *J. Chem. Phys* **27** (1957) 1208; *J. Chem. Phys* **33** (1960) 1439; W.G Hoover and R.M Ree *J. Chem. Phys* **49** (1968) 3609
7. B.J Alder and T.E Waiwright, *Phys. Rev.* **127** (1962) 359
8. J.A. Zollweg and G.V. Chester, *Phys. Rev.* **B46** (1992) 11186; J. Lee and K.J. Strandburg, *Phys. Rev.* **B46** (1992) 11191
9. J.P Hansen and L Verlet *Phys. Rev.* **184** (1969) 151;
10. W. Vermhlen and N. Ito *Phys. Rev.* **E51** (1995) 4325
11. A. Awazu, To appear in *Phys. Rev. E* (cond-mat/0006466)
12. R.Tehver, F.Toigo, J.Koplik and J.R.Banavar, *Phys. Rev.* **E57** (1998) 57

FIGURES

Fig. 1. Illustration of two particles system in a box with a moving wall (right) and energy sources (left)

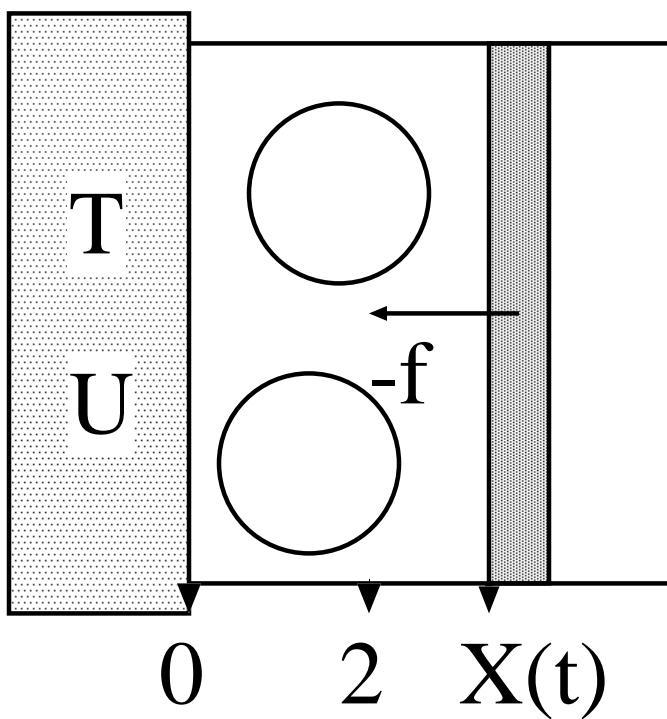
Fig. 2. Probability distribution of the position of right wall $X(t)$ (PD) for typical values f with, respectively, when (a) $Y = 4.5$ (Middle $f = 0.1725$), (b) $Y = 5.0$ (Middle $f = 0.1345$), and (c) $Y = 5.5$ (Middle $f = 0.1225$) under $T = 0.1$ and $U = 0$.

Fig. 3. Probability distribution of the position of right wall $X(t)$ (PD) for typical values U and $f = 1$ with, respectively, (a) $Y = 4.5$ with $T = 0.1$ (Middle $U = 1.14$), (b) $Y = 4.5$ with $T = 0.4$ (Middle $U = 0.665$), (c) $Y = 5.5$ with $T = 0.1$ (Middle $U = 1.925$), and (d) $Y = 5.5$ with $T = 0.4$ (Middle $U = 1.25$).

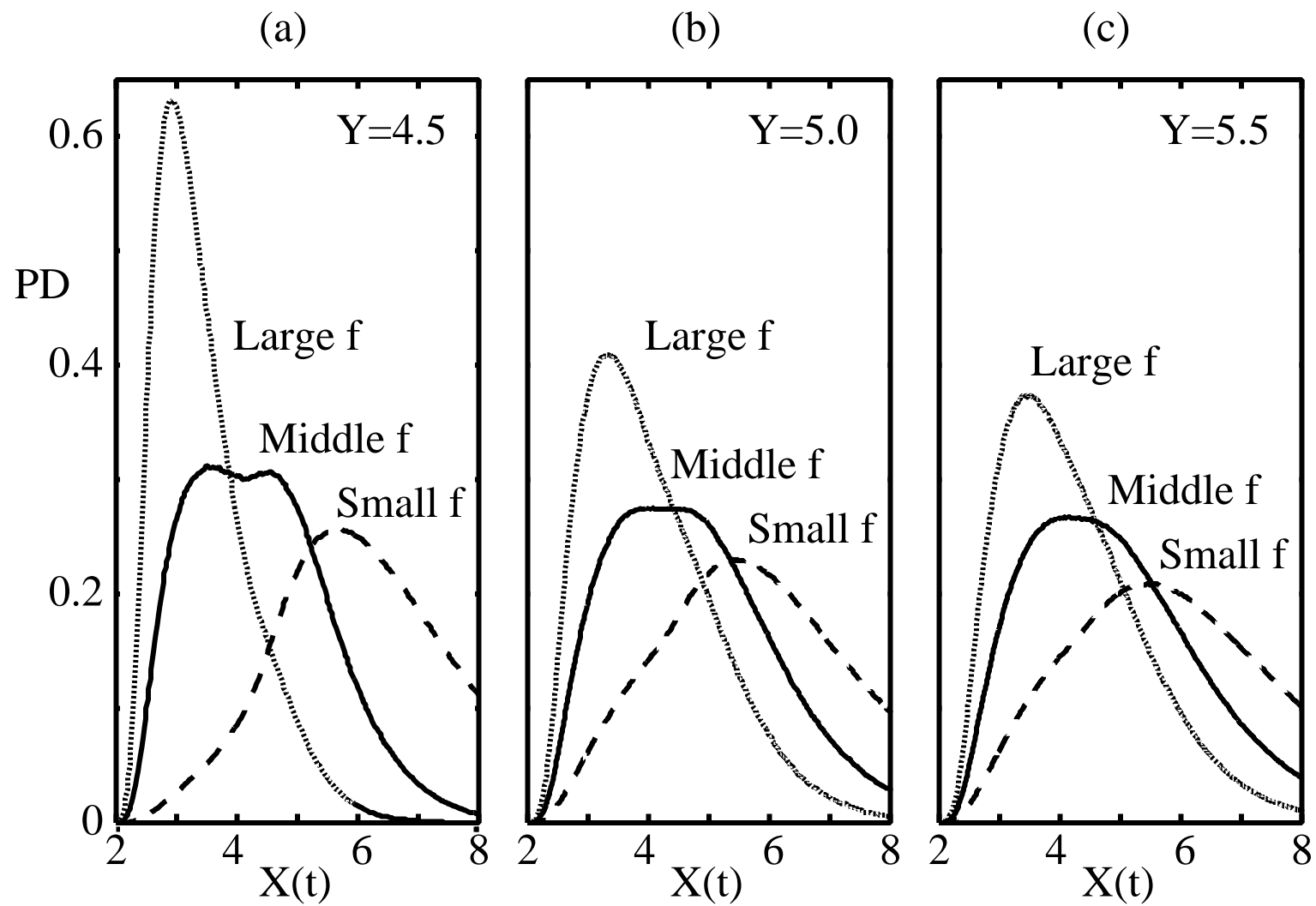
Fig. 4. Relations between (a) U and m and (b) U and F_{ex} for typical values T ($T = 0.06, 0.24$ and 0.42) with $Y = 5.0$ and $f = 1$

Fig. 5. Relations between m and R (F_{ex}) for typical values T with, respectively, (a) $Y = 5.0$ ($T = 0.06, 0.24$ and 0.42) and (b) $Y = 4.5$ ($T = 0.05, 0.21$ and 0.37) ($f = 1$)

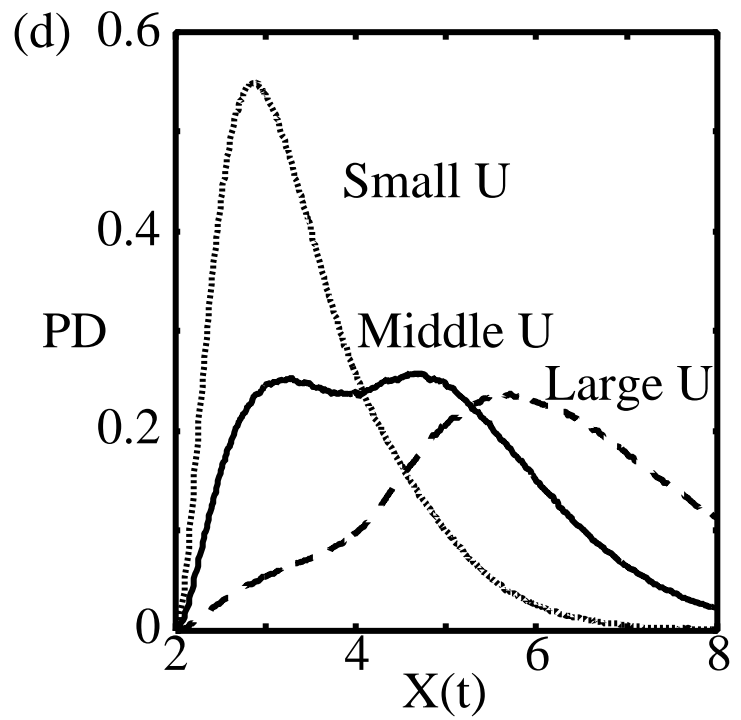
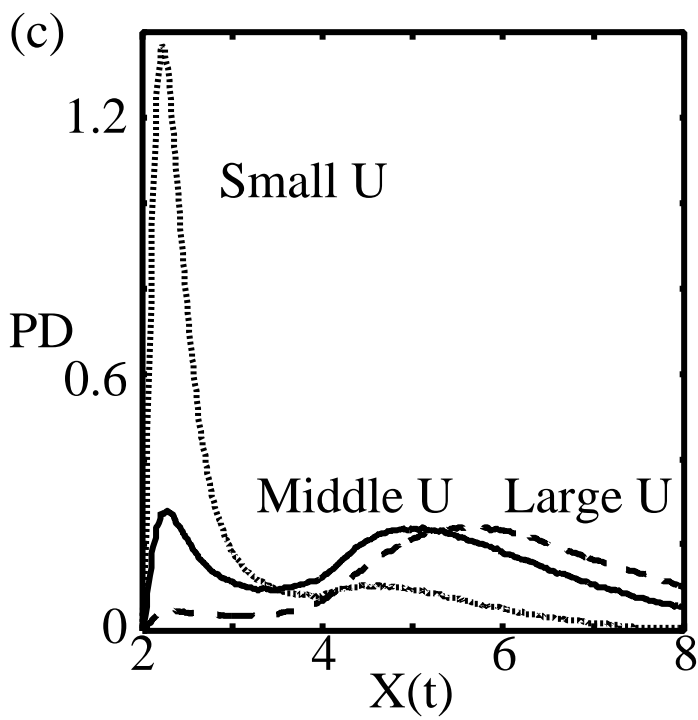
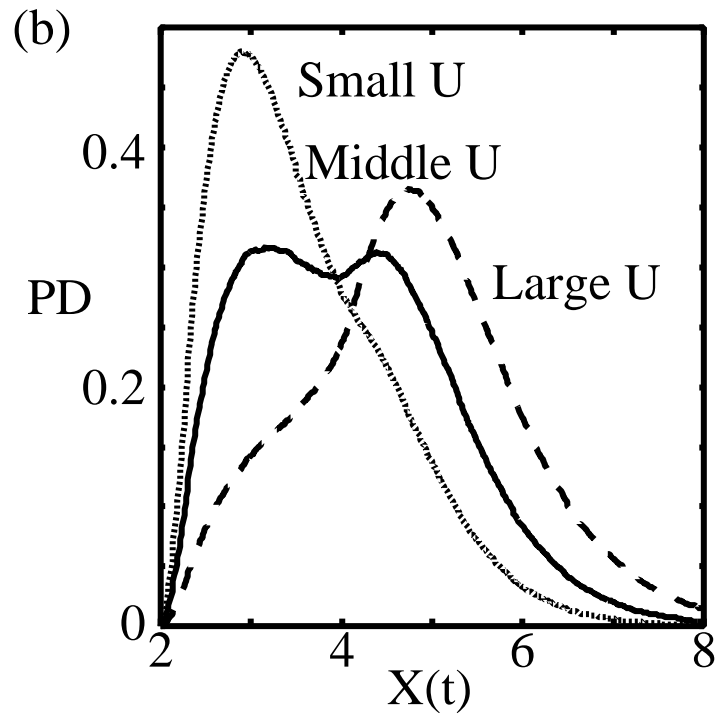
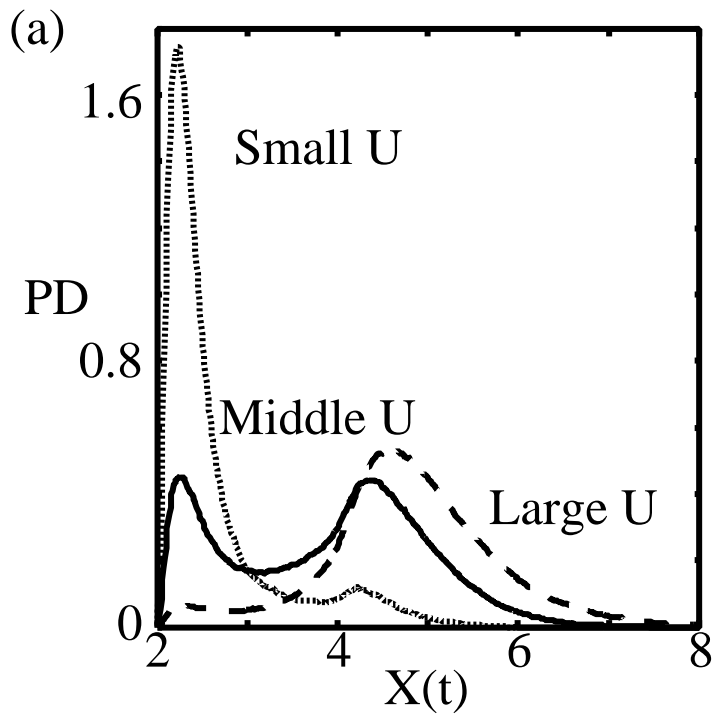
Fig. 6. Relations between (a) m and μ , and (b) f and μ , for typical values T ($T = 2^{-5}, 2^{-4}$ and 2^{-3}) with $Y = 5.0$ and constant U ($U = 2.0$).

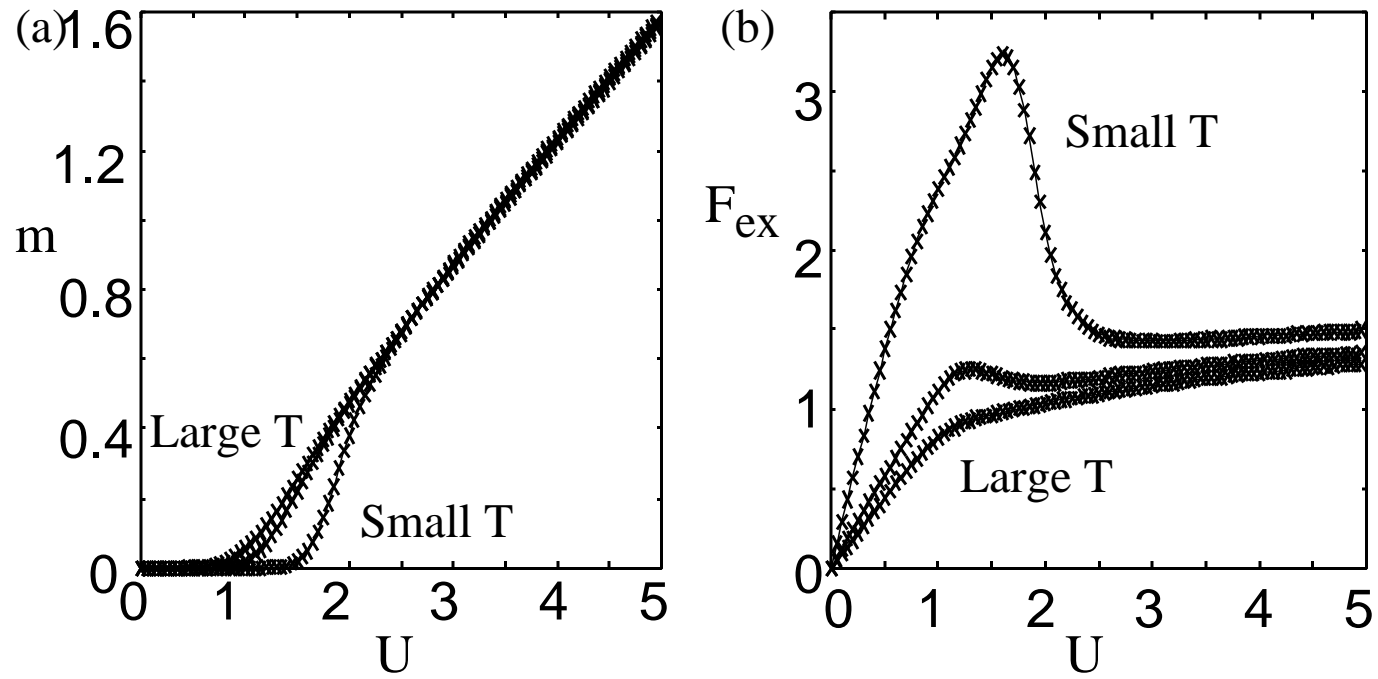


A. Awazu Figure 1

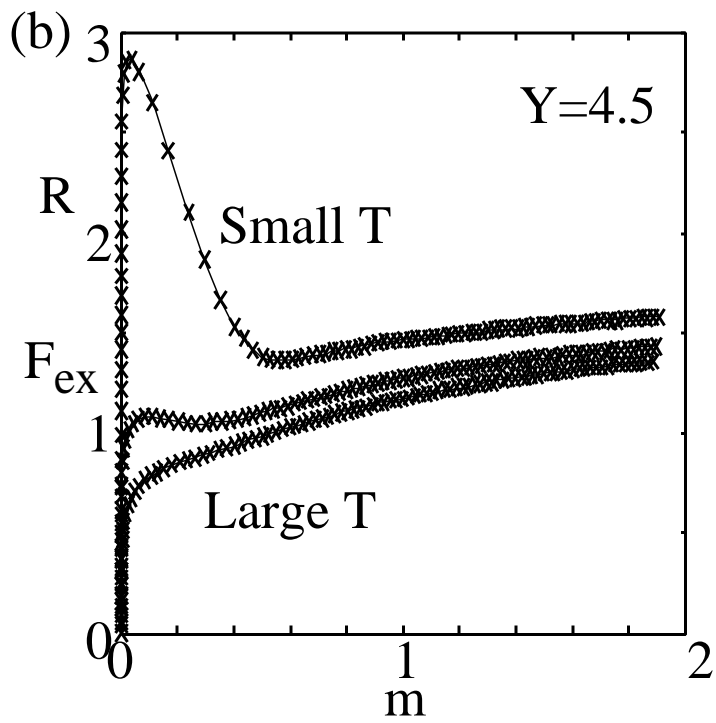
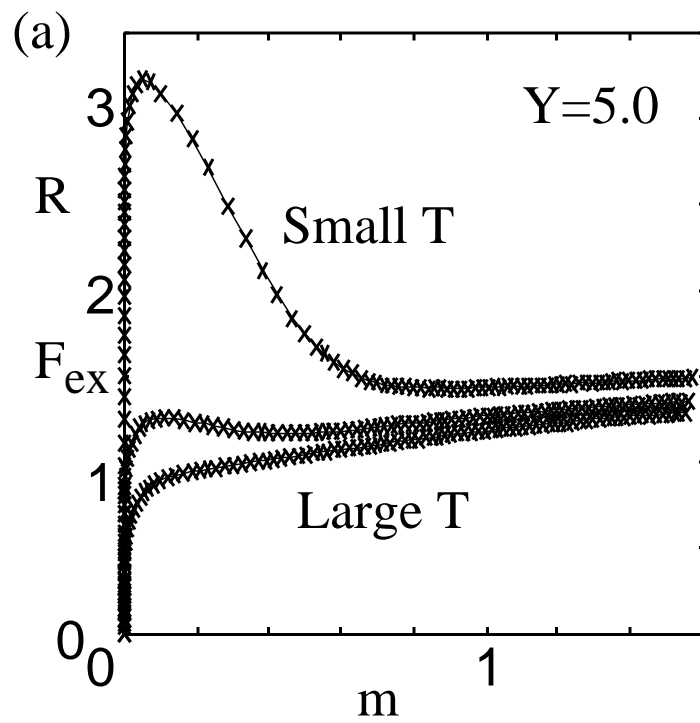


A. Awazu Figure 2

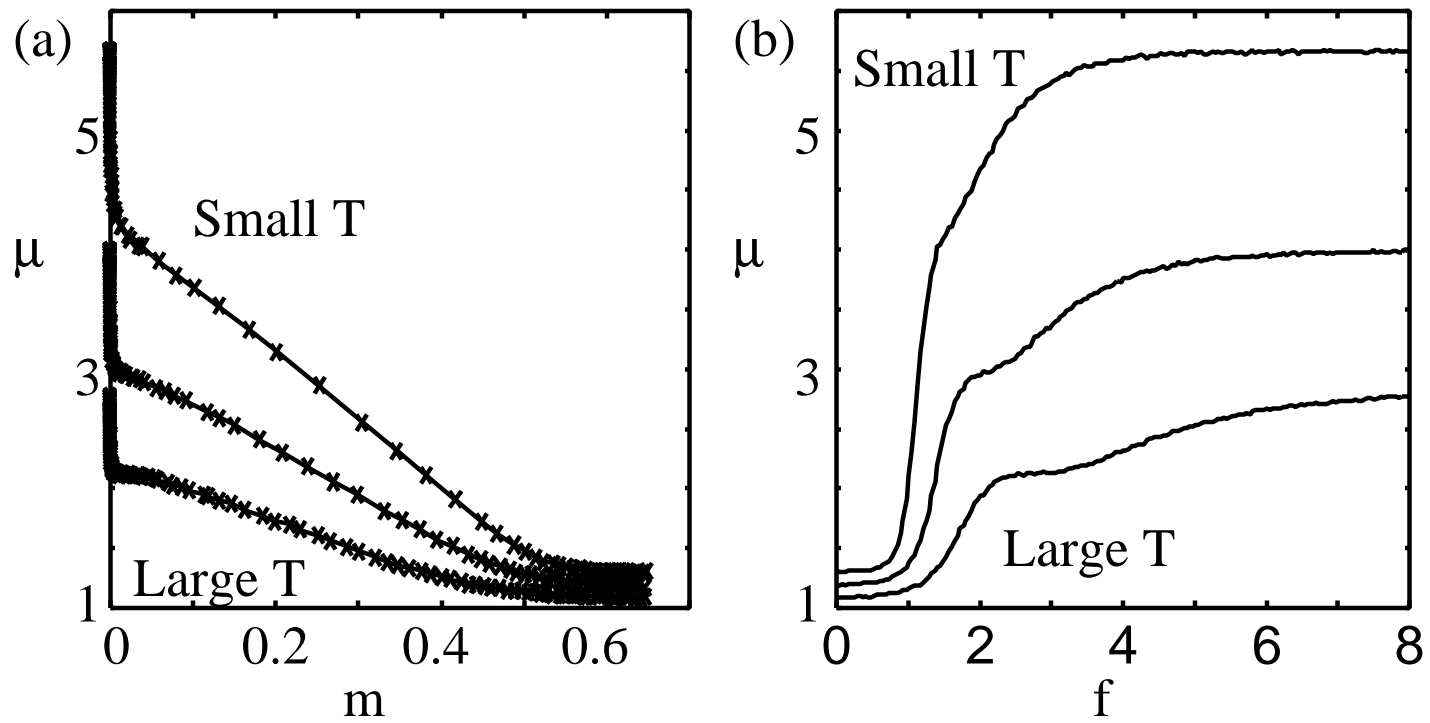




A. Awazu Figure 4



A. Awazu Figure 5



A. Awazu Figure 6